

EFFECT OF MORPHOLOGY ON DENSIFICATION

STUDY OF NANO – HYDROXYAPATITE

Presented by :-

Kunal Kumar Tanty

108CR054

NIT Rourkela

PROJECT THESIS SUBMITTED IN PARTIAL FULFILMENT OF THE REQUIREMENTS

FOR THE DEGREE OF

BACHELOR OF TECHNOLOGY



Department of Ceramic Engineering

National Institute of Technology, Rourkela, Orissa - 769008

CERTIFICATE

This is to certify that this thesis entitled , “EFFECT OF MORPHOLOGY ON DENSIFICATION STUDY OF NANO – HYDROXYAPATITE”, submitted by Mr Kunal Kumar Tanty in partial fulfilment of the requirement of the award of Bachelor of Technology Degree in Ceramic Engineering at National Institute of Technology, Rourkela is an authentic work carried out by him under my supervision and guidance.

To the best of my knowledge, the matter embodied in the thesis has not been submitted to any other university/institute for the award of Degree or Diploma.

ROURKELA

Dr. Debasish Sarkar

Department of Ceramic Engineering

National Institute of Technology,

Rourkela, Orissa - 769008

Date:

Acknowledgements

I would like to express my heartfelt thanks and gratitude to Professor Debasish Sarkar, Department of Ceramic Engineering, NIT Rourkela, my guide and my mentor, who was with me during every stage of the work; and whose guidance and valuable suggestions has made this work possible.

Further, I would also like to thank all the faculty members and staff of Department of Ceramic Engineering, NIT Rourkela for their invaluable support and help during the entire project work.

I would further like to thank all the research scholars, especially Mr. Sanjay Swain, Mr. Ganesh kumar sahu and last but not the least Miss Geetanjali parida, for their round the clock help and support during the entire project work.

Last but not the least I want to thank almighty lord for the successful completion of the project work.

Kunal Kumar Tanty
Roll No- 108CR054

Abstract

Spherical, rod and fibrous morphology of Hydroxyapatite (HA) nanoparticles were considered to understand the densification behaviour at high temperature. Thermal analysis of as-received HA nanoparticles confirmed the phase transformation temperature for different morphologies. The phase stability was strictly deepened on morphology of HA nanoparticles. X – ray diffraction (XRD) pattern and Fourier transformation Infrared (FTIR) was studied to evaluate the crystal structure, phase and purity for different calcined powders and their sintered specimens. Spherical, rod and fibrous nano-HA morphology were stable up to 1200°C, 700°C and 1000°C, respectively, which were decomposed to beta tricalcium phosphate (β – TCP) beyond these critical temperatures. Dilatometric study of all green specimens prepared from such nanoparticles was conducted up to 1250°C to synchronize the sintering temperature. The densification behaviour was dramatically changed with respect to morphology when sintered at different temperatures; such as 700°C, 900°C, 1000°C, 1250°C, respectively. Scanning electron microscopic (SEM) image, apparent porosity and relative density were studied to justify the densification behaviour of HA nanoparticles.

Table of Contents

EFFECT OF MORPHOLOGY ON DENSIFICATION STUDY OF NANO – HYDROXYAPATITE	i
Acknowledgements	ii
Abstract.....	iii
Table of Contents	iv
LIST OF FIGURES	vi
LIST OF TABLES	vi
Chapter 1	1
INTRODUCTION.....	1
1.1 HYDROXYAPATITE.	2
1.1.1 STRUCTURE.....	3
1.1.2 APPLICATIONS.....	4
Chapter 2	5
LITERATURE REVIEW.....	5
2.1 DENSIFICATION OF HYDROXYAPATITE.....	6
2.2 MORPHOLOGICAL STUDIES	6
2.3 STRUCTURE EFFECTS	7
2.4 OBJECTIVE.....	8
Chapter 3	9
EXPERIMENTAL	9
3.1 PELLETIZATION	10
3.2 SINTERING AT DIFFERENT TEMPERATURES:-	10
3.3 CHARACTERISATION.....	11
3.3.1 DSC/TG.....	11
3.3.2 XRD	11
3.3.3 FTIR	11
3.3.4 DILATOMETRIC ANALYSIS	12
3.3.5 SEM ANALYSIS	12
3.3.6 BULK DENSITY AND APPARENT POROSITY MEASUREMENT	12
Chapter 4	13
4.1 THERMAL ANALYSIS OF HYDROXYAPATITE	14
4.1.1 THERMAL ANALYSIS OF NANO SPHERICAL HYDROXYAPATITE.....	14
4.1.2 THERMAL ANALYSIS OF NANO FIBRE HYDROXYAPATITE.....	15

4.2	X-RAY DIFFRACTION AFTER SINTERING	16
4.2.1	NANO – SPHERICAL HYDROXYAPATITE	16
4.2.2	NANO – ROD HYDROXYAPATITE.....	17
4.2.3	NANO-FIBRE HYDROXYAPATITE	18
4.3	FTIR SPECTROSCOPY TO CHECK PURITY.....	19
4.4	DILATOMETRIC STUDY OF HYDROXYAPATITE.....	20
4.5	SEM ANALYSIS	21
4.5.1	NANO –SPHERICAL HYDROXYAPATITE	21
4.5.2	NANO ROD HYDROXYAPATITE.....	22
4.5.3	NANO FIBRE HYDROXYAPATITE.....	23
4.6	BULK DENSITY OF DIFFERENT MORPHOLOGIES	24
4.7	APPARENT POROSITY OF DIFFERENT MORPHOLOGIES.....	25
4.8	BULK DENSITY AND APPARENT POROSITY AS A FUNCTION OF TEMPERATURE.....	26
4.8.1	NANO SPHERICAL HYDROXYAPATITE	26
4.8.2	NANO ROD HYDROXYAPATITE.....	26
4.8.3	NANO FIBRE HA	27
Chapter 5	28
CONCLUSION	28
REFERENCES	30

LIST OF FIGURES

Figure 1 HA crystal on matrix [1].....	2
Figure 2 Crystal Structure [2]	3
Figure.3 Hydroxyapatite morphologies : (a) spherical (b) rod shaped (c) fibre shaped [3,4,5]	3
Figure 4 DSC/TG of Nano Spherical HA	14
Figure 5 DSC/TG of Nano fibre HA	15
Figure 6 XRD of Nano-Spherical HA.....	16
Figure 7 XRD of Nano Rod HA	17
Figure 8 XRD of Nano fibre HA	18
Figure 9 IR Spectrum composite of nano - (a) spherical (b) rod (c) fibre	19
Figure 10 Dilatometric study of Nano HA.....	20
Figure 11 SEM of Sintered Nano-spherical HA at 1250°C	21
Figure 12 SEM of sintered Nano-spherical HA.....	22
Figure 13 (a) SEM of calcined Nano-fibre HA (b) SEM of raw Nano-fibre HA.....	23
Figure 14 BD composite of HA	24
Figure 15 AP composite of HA.....	25
Figure 16 BD vs AP of Nano-spherical HA	26
Figure 17 BD vs AP of Nano-rod HA.....	27
Figure 18 BD vs AP of Nano-fibre HA	27

LIST OF TABLES

Table 1 Sintering temperatures	10
--------------------------------------	----

Chapter 1

INTRODUCTION

1.1 HYDROXYAPATITE.

Hydroxyapatite(HA) is a naturally occurring mineral form of calcium apatite with the formula $\text{Ca}_5(\text{PO}_4)_3(\text{OH})$ which can be written as $\text{Ca}_{10}(\text{PO}_4)_6(\text{OH})_2$ to denote that the crystal unit cell comprises of two entities. HA material has been clinically applied in many areas of density and orthopaedics because of its excellent osteoconductive and bio active properties. It is the main inorganic constituent of bones in humans. Synthetic HA is successful in hard tissue surgery and undergoes bonding osteogenesis. However it has low load bearing application as because of its poor mechanical properties. In present scenario morphologies are playing a vital role in the mechanical properties of the body, also the microstructure. Nano structured HA with different morphologies like spherical, rod and fibre are found to characterise HA in different application.



Figure 1 HA crystal on matrix [1]

HA on sintering decomposes to anhydrous calcium phosphate such as Tri calcium phosphate(TCP),at higher temperature as a result of dehydroxylation beyond a critical point. An important property of HA is that it is chemically stable for long periods of time. Different densification behaviour of HA particles were observed in the temperature range of 1100 – 1300°C. While porous HA is advantageous promoting bone in growth and dense HA is used in load bearing application.

1.1.1 STRUCTURE

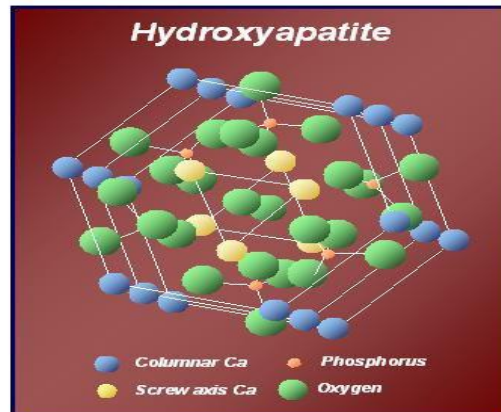


Figure 2 Crystal Structure [2]

Hydroxylapatite is the hydroxyl end member of the complex apatite group. The OH^- ion can be replaced by fluoride, chloride or carbonate, producing fluoroapatite or chloroapatite. It crystallises in the hexagonal crystal system. Pure HA powder is white. Naturally occurring apatites can, however, also have brown, yellow, or green colorations, comparable to the discolorations of dental fluorosis.

We are concerned with the following three morphologies as shown in figure 3.

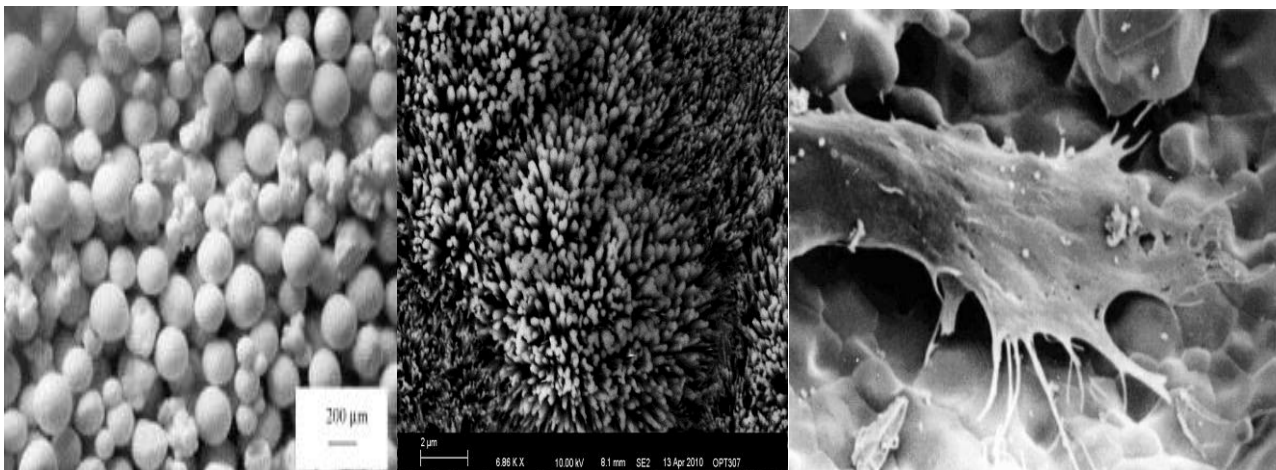


Figure.3 Hydroxyapatite morphologies : (a) spherical (b) rod shaped (c) fibre shaped [3,4,5]

1.1.2 APPLICATIONS

HA can be found in teeth and bones within the human body. Commonly used as a filler to replace amputated bone or as a coating to promote bone in growth into prosthetic implants, although many other phases exist with similar or even identical chemical makeup, the body responds much differently to them. Coral skeletons can be transformed into HA by high temperatures. Their porous structure allows relatively rapid growth at the expense of initial mechanical strength. The high temperature also burns away any organic molecule such as proteins, preventing an immune response and rejection.

Chapter 2

LITERATURE REVIEW

2.1 DENSIFICATION OF HYDROXYAPATITE.

S. Jaasri et al presented report on the effect of densification on the mechanical properties of HA. [6] The densification study was done at range of 1000 °C -1300 °C. Further XRD and SEM were used to verify the micro structural transformation. It was found that the sintering temperature and particle size influence the densification and mechanical properties strongly. This showed the mechanical property of HA being sensitive to densification

CY tan et al followed the method of microwave rapid sintering which was found to be beneficial in terms of densification and mechanical properties. [7] This property achieved a theoretical density of 96% at a sintering temperature of 1100 °C maintaining its microstructure. However further sintering the body were not governed by density effect but were associated with grain size effect. The sinterability of nano HA was studied. The xrd patterns of the sintered HA compacts fired between 1000 ° C and 1250 °C were studied. The decomposition of HA was not observed throughout the sintering process. However grain coarsening was observed above 1200 °C. Regardless of sintering methods there existed a co-relation between hardness & grain size in HA. The hardness of HA would start decreasing at certain critical grain size limit despite high bulk density.

2.2 MORPHOLOGICAL STUDIES

Ashis Banerjee et al studied the effect of powder morphology on densification at 1250 ° c with different amount of rod shaped and spherical nano –powders. [8] It was observed that an increase in high aspect ratio powder content in the compacts decreased sintered density under pressure less sintering conditions. Sometimes no nano scale morphology could be retained in sintered

microstructure. However in case of simulated body fluid showed formation of apatite layer on entire surface of compacts made with spherical and rod-shaped particles.

Microhardness was decreased due to the addition of rod-shaped particle and fracture toughness increased with rod-shaped particle additive to spherical nanopowder. It was also found that due to grain growth no rod shaped particles were pressed after high temperature sintering with the formation of dense apatite layer.

DyCheang et al examined the effect of powder morphology on the tensile properties of polymer-HA composite [9]. Experimental findings showed that surface morphology and structural integrity of HA have considerable influence on properties of composites. HA with rough surfaces promoted mechanical interlocking and also improved the interfacial bonding. Relatively lower tensile strength was achieved by porous agglomerated HA powder.

2.3 STRUCTURE EFFECTS

Hala Zreiqat et al studied the influence of hydroxylapatite nanoparticle shape and size on biphasic calcium phosphate scaffold and found that highly porous scaffold showed maximum compressive strength and the nano composite coated scaffold of needle shaped HA showed strong osteoblast profile, which shows that scaffold possessed improved mechanical and biological properties which proves essential in application of bone tissue regeneration[10].

E.Landi et al prepared and characterised HA powders with different crystallinity degrees. [11]Now densification and densification mechanism were studied at a range of 700-1250 °C .The effect of different powder features with calcinations effect were evaluated .powder characterised by lowest crystallinity had highest densification. The physio-chemical features of different powders affect the

densification behaviour and grain growth is stimulated due to grain boundary diffusion process, which improves densification. The whole process is time and temperature dependent.

Irina et al characterised the composite by FTIR spectroscopy with X-ray diffraction and scanning electron microscopy, which showed typical absorption bands for ACand HA confirming the formation of composite. [12]

The XRD patterns revealed the characteristics peaks of low crystalline HA. The SEM micrographs shared the morphology of pre mineralised and composite samples and hence estimated the HA particles.

G.Muralitharan et al studied the effects of sintering temperature on properties of HA. [13]It showed that the sintering of HA resulted in microstructure and the properties were influenced by characterisation and impurities of raw material and also depended on the thermal history during the fabrication process. This work was concerned on effect of grain size on relative density and hardness .Here is iso-statically pressed HA was sintered at temperature ranging from 1000 °C to 1450 ° C and it was found that upto 1250°C the material composed pure HA phase. Porosity and grain size played an important role in determining the properties of sintered HA.

2.4 OBJECTIVE

- To understand the phase stability of different morphologies at a particular level of temperature
- To understand the densification behaviour with respect to temperature, morphologies and phase stability.

Chapter 3

EXPERIMENTAL

3.1 PELLETIZATION

0.5 gm each of nano spherical and nano fibre HA and 0.3 gm of nano rod HA were weighed for preparing pellets. A few drops of poly-vinyl alcohol (PVA 2%) in an agate mortar was mixed with each composition. Keeping the dwell time to 120 seconds, powder compositions were then pressed in a circular die of diameter 12mm at 4 ton pressure. For dilatometric test 1.0 gm each of nano spherical and nano fibre HA and 0.5 gm of nano rod HA were weighed for preparing pellets. Keeping the dwell time upto 120 second and pressure upto 4 ton pressing was done to form bars.

3.2 SINTERING AT DIFFERENT TEMPERATURES:-

After pressing the green samples were fired at 400°C, 700°C,900°C,1000°C,1250°C for 2 hrs. Firing were done in electric chamber furnace ,pit furnace, initially kept on hold at 650°C for 1 hr for complete binder burnout and then soaked at firing temperature for 2 hr. Heating rate was kept to 3°Cmin⁻¹.The fired product was then cooled at room temperature and bulk density was calculated.

Table 1Sintering temperatures

Morphology	Sintering temperatures					
	Raw(80°C)	400°C	700°C	900°C	1000°C	1250°C
Spherical	Y	N	N	Y	Y	Y
Rod	Y	Y	Y	Y	Y	Y
Fibre	Y	N	Y	Y	Y	Y

3.3 CHARACTERISATION

3.3.1 DSC/TG

The DSC/ TG thermal analysis were conducted in a Netzsch 449C Thermal Analyser. The samples were heated in flowing argon (Ar) gas atmosphere keeping the heating rate of 5°C/min and 10°C/min in the temperature range of 0°C to 1250°C . The weight loss measurements were also done in the same instrument.

3.3.2 XRD

The X-Ray Diffraction pattern of raw and sintered samples at 400°C, 700°C, 900°C, 1000°C, 1250°C of each nano spherical, nano rod and nano fibre morphology HA were obtained in Philips X-Ray Diffractometer (pan-analytical PW 1730) with nickel filtered Cu K α radiation ($\lambda=1.5406 \text{ \AA}$) at 40 kV and 30 mA. The scanning rate was kept at 0.04 sec⁻¹ within a continuous scanning range of 20° to 80°.

3.3.3 FTIR

The presence of the concerned functional groups at raw stages was studied by Fourier Transform Infrared Spectroscopy, FTIR (perkin Elmer US). The FTIR spectra were taken on the sample powders. The binders were pressed to a circular-disc (10 mm \varnothing) by mixing small quantity of powder with Potassium bromide (KBr). The samples scanning wave number range was kept at 4000-400 cm⁻¹.

3.3.4 DILATOMETRIC ANALYSIS

The shrinkage behaviour were obtained by NETZSCH dilatometer model DIL 402 C with a sample length of 10mm and thickness of 2mm bar pellet. The heating rate was kept constant at $10^{\circ}\text{Cmin}^{-1}$ with firing temperature beginning from room temperature to 1300°C . The atmosphere inside the dilatometer was N_2 atmosphere

3.3.5 SEM ANALYSIS

Raw samples in form of powder and sintered pellets at 400°C , 700°C , 900°C , 1000°C , 1250°C for 2 hrs were characterised in order to determine the morphological changes and micro structural changes as a result of densification after sintering.

3.3.6 BULK DENSITY AND APPARENT POROSITY MEASUREMENT

To measure bulk density and apparent porosity of sintered HA pellets, the dry weight of pellets was first measured. Then they were soaked in kerosene inside a beaker and were evacuated till all the air bubbles vanished. After that they were kept inside dessicator vacuum for few hours. After removing from the vacuum the suspended weight and soaked weight of the samples were calculated. In order to obtain bulk density (B.D.) the following formula was used:

$$\text{B.D.} = (\text{dry weight}) * (0.813) / (\text{soak weight} - \text{suspended weight})$$

To obtain apparent porosity (A.P.) in % the formula used is:

$$\text{A.P.} = (\text{soak weight} - \text{dry weight}) * 100 / (\text{soak weight} - \text{suspended weight})$$

Chapter 4

RESULTS AND DISCUSSION

4.1 THERMAL ANALYSIS OF HYDROXYAPATITE

4.1.1 THERMAL ANALYSIS OF NANO SPHERICAL HYDROXYAPATITE

Figure 4 shows the DSC/ TG study of the nano spherical HA at 5°C/min showing significant weight loss taking place only upto around 1250°C. The plotted curve shows endothermic peaks at 100 °C due to dehydroxylation of absorbed moisture leading to mass loss. Broad exothermic peaks at 600°C corresponds to the decomposition of carbonate resulting in significant weight loss and also these exothermic peak at higher temperature corresponds to the crystallisation and oxidation of the residual mass .TG curve shows weight loss of 12%, as a result of PVA burnout and moisture loss followed by the weight loss added by decomposition of phases.

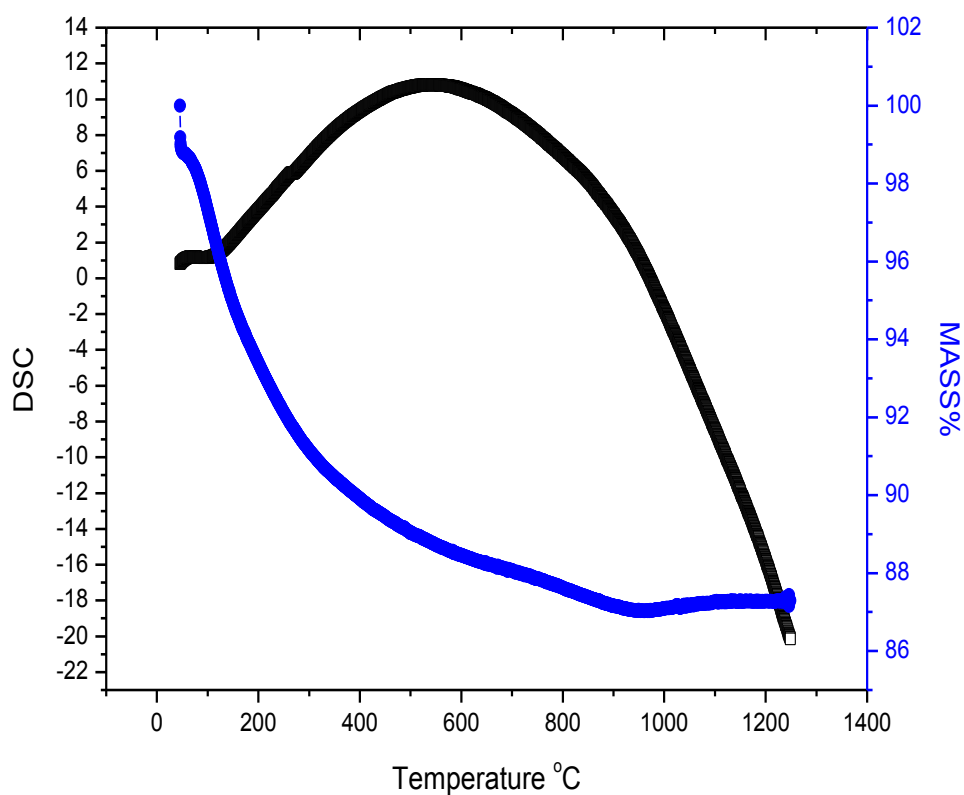


Figure 4 DSC/TG of Nano Spherical HA

4.1.2 THERMAL ANALYSIS OF NANO FIBRE HYDROXYAPATITE

Figure 5 shows the DSC/ TG study of the nano spherical HA at 5°C/min showing significant weight loss taking place only upto around 1250°C. The plotted curve shows endothermic peaks at 100 °C due to dehydroxylation of absorbed moisture leading to mass loss.

Broad exothermic peaks at 600°C and 1000°C corresponds to decomposition of carbonate resulting in significant weight loss and also these exothermic peak at higher temperature corresponds to the crystallisation and oxidation of the residual mass .TG curve shows weight loss of 18% as a result of PVA burnout and moisture loss followed by the weight loss added by decomposition of phases.

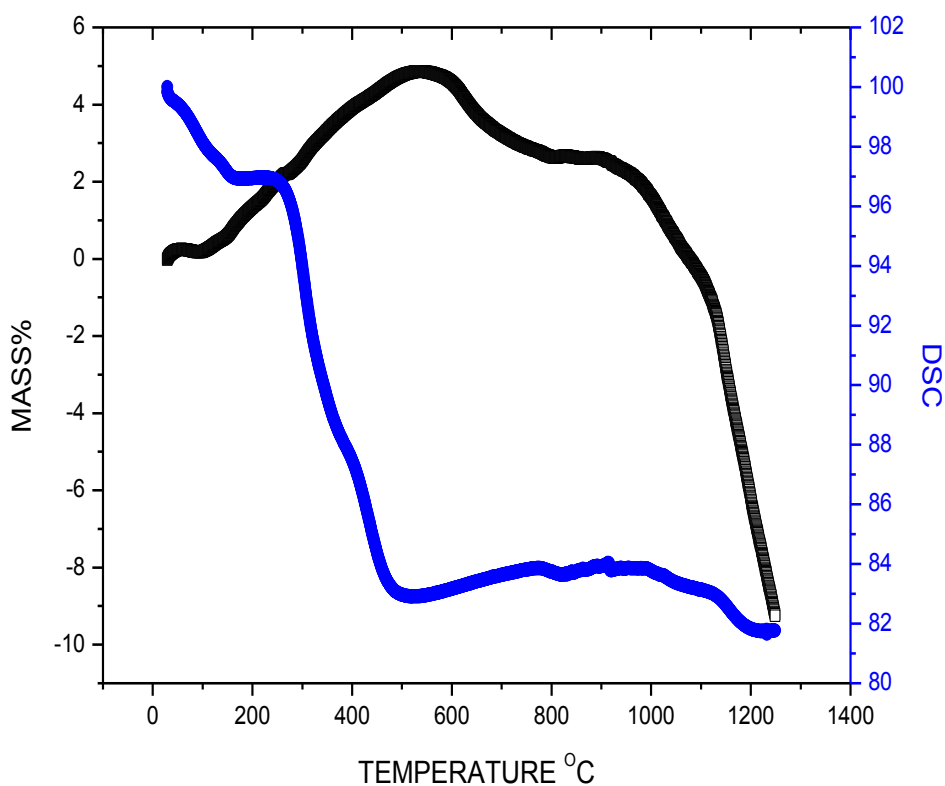


Figure 5 DSC/TG of Nano fibre HA .

4.2 X-RAY DIFFRACTION AFTER SINTERING

4.2.1 NANO – SPHERICAL HYDROXYAPATITE

The XRD of Nano Spherical HA pellets sintered at concerned temperatures is shown in Figure 6. Initially at raw stages ultra pure HA phases are found. As the temperature is increased the decomposition of HA begins at very later stages. Nano spherical HA being highly stable among the rest, retains the pure HA phase upto temperature of 1100°C. At 1250°C minor decomposition of HA to TCP is observed.

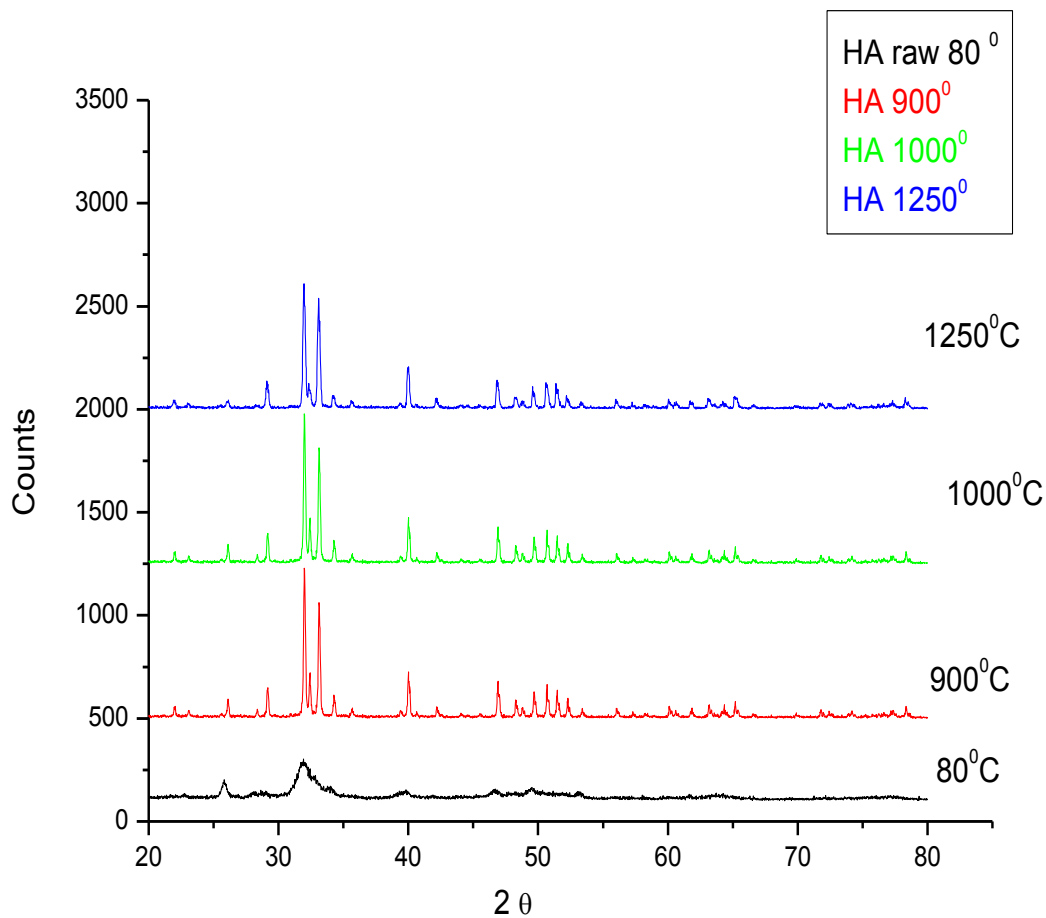


Figure 6 XRD of Nano-Spherical HA

4.2.2 NANO – ROD HYDROXYAPATITE

The XRD of Nano Rod HA pellets sintered at concerned temperatures is shown in Figure 7. Initially at raw stages ultra pure HA phases are found. As the temperature is increased the decomposition of HA begins at later stages. Nano rod HA being stable upto 1000°C, retains the pure HA phase upto temperature of 1000°C and then HA starts decomposing to TCP.

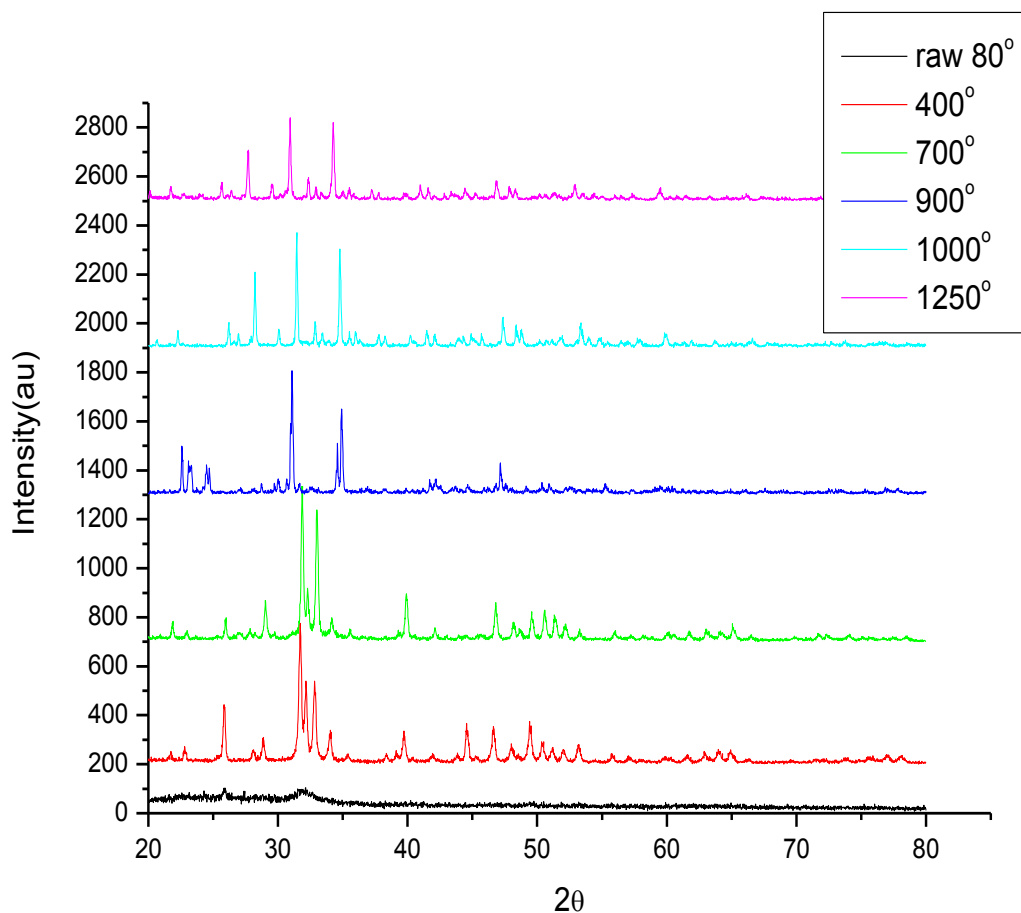


Figure 7 XRD of Nano Rod HA .

4.2.3 NANO-FIBRE HYDROXYAPATITE

The XRD Nano Fibre HA pellets sintered at 900 ° C ,1000 ° C ,1250 ° C temperatures is shown in Figure 8. Initially at raw stages ultra pure HA phases are found. As the temperature is increased the decomposition of HA begins at later stages .Nano fibre HA being stable upto700°C, retains the pure HA phase upto temperature of 700°C and then HA starts decomposing to TCP. First β TCP is obtained then α TCP follows.

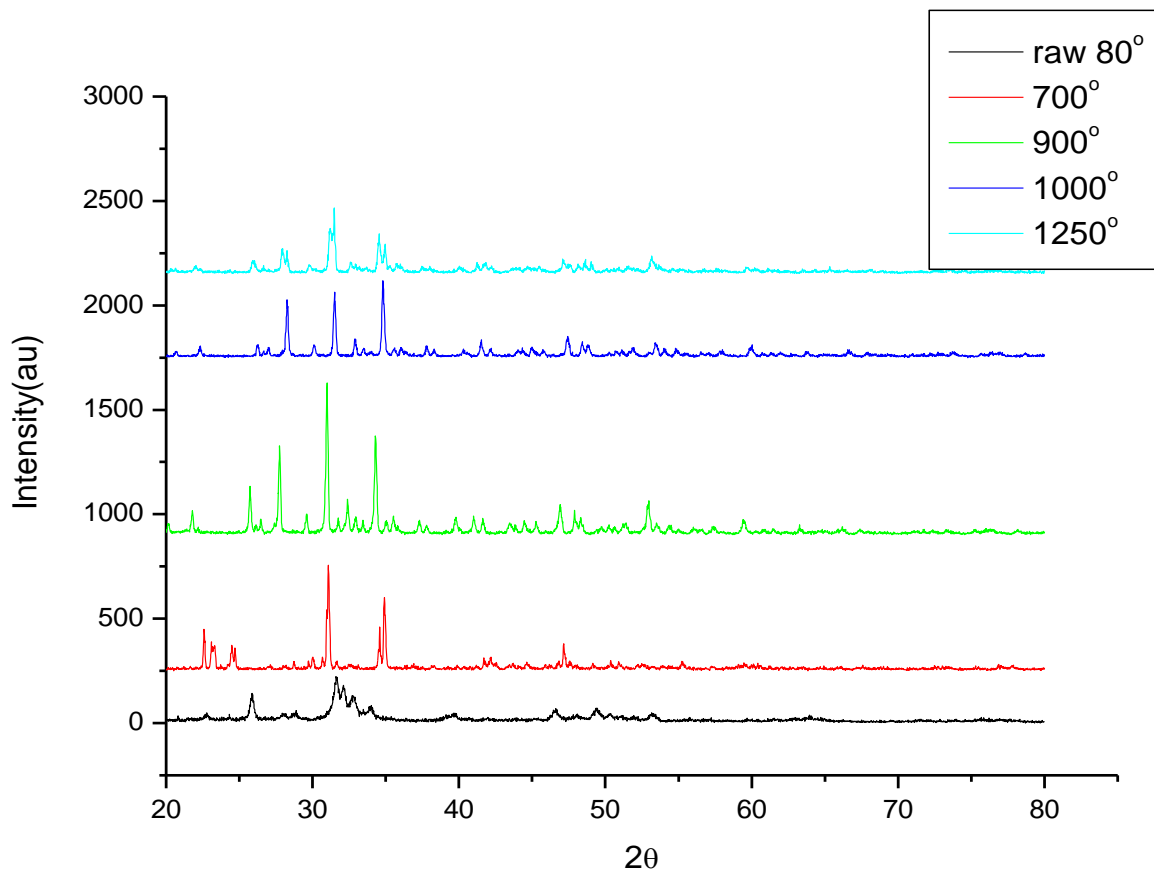


Figure 8 XRD of Nano fibre HA

4.3 FTIR SPECTROSCOPY TO CHECK PURITY

The Figure 9 shows the FTIR spectra of the three nano morphologies HA, showing all the characteristics bands for HA in its raw stages before thermal treatment. The asymmetric stretching and bending modes of PO_4^{3-} ion were detected at around 650cm^{-1} for nano-spherical, nano-rod and nano fibre HA. PO_4^{3-} ions were also detected at 1000cm^{-1} respectively. The liberation and stretching mode of OH^- were detected at 600cm^{-1} and 3500cm^{-1} respectively. The stretching vibrations ascribed to CO_3^{2-} ions at around 1500cm^{-1} . This indicates that carbonate group is incorporated into the apatite structure. However nano-fibre HA is found to liberate less CO_3^{2-} . This study shows the different stages of decomposition completion. Broad peaks are found showing the presence of water or alcohol, this part contains excess of OH group.

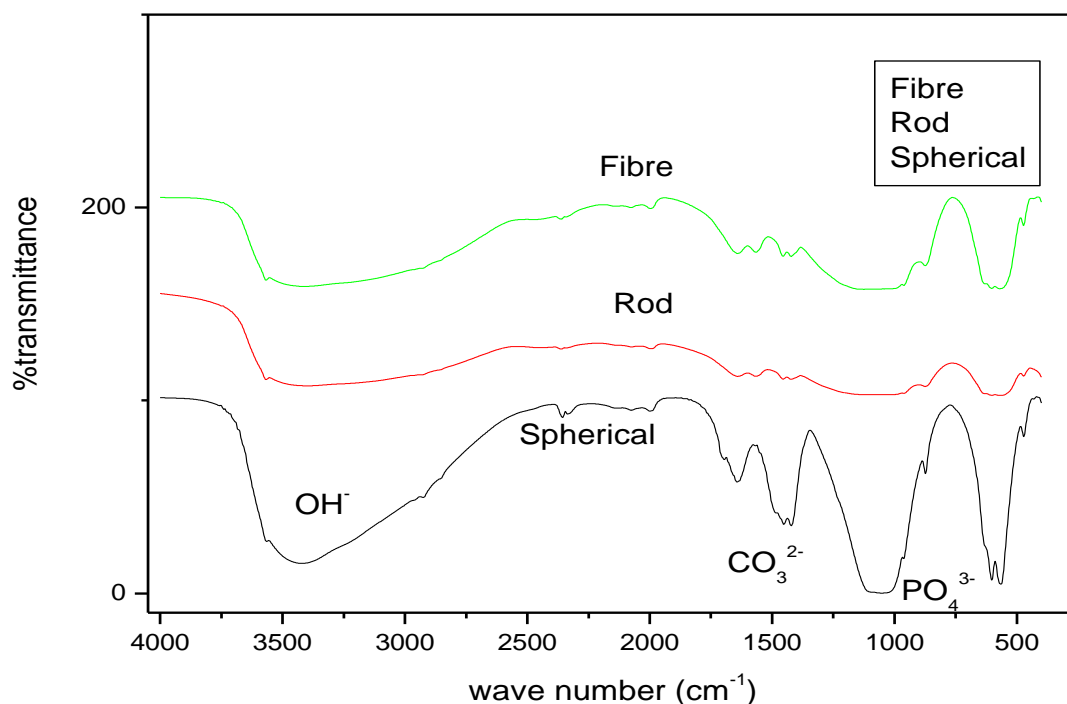


Figure 9 IR Spectrum composite of nano - (a) spherical (b) rod (c) fibre

4.4 DILATOMETRIC STUDY OF HYDROXYAPATITE

Figure 10 shows the shrinkage behaviour of the three concerned morphologies of HA operated upto a temperature of 1300 ° C. Nano spherical HA started shrinking at an on set temperature of 900 ° C and continued to shrink upto 1300 ° C. In cases of nano rod HA shrinking starts at an on set temperature of 1200 ° C and continues upto later stages. For nano fibre HA shrinking starts at an on set temperature of 1100 ° C. The initial shrinkages occurring are due to the decomposition of PVA and moisture loss. The shrinkage in case of nano-spherical HA is found to be 0.16, that for nano-rod HA is 0.06 and for nano-fibre HA is 0.03.

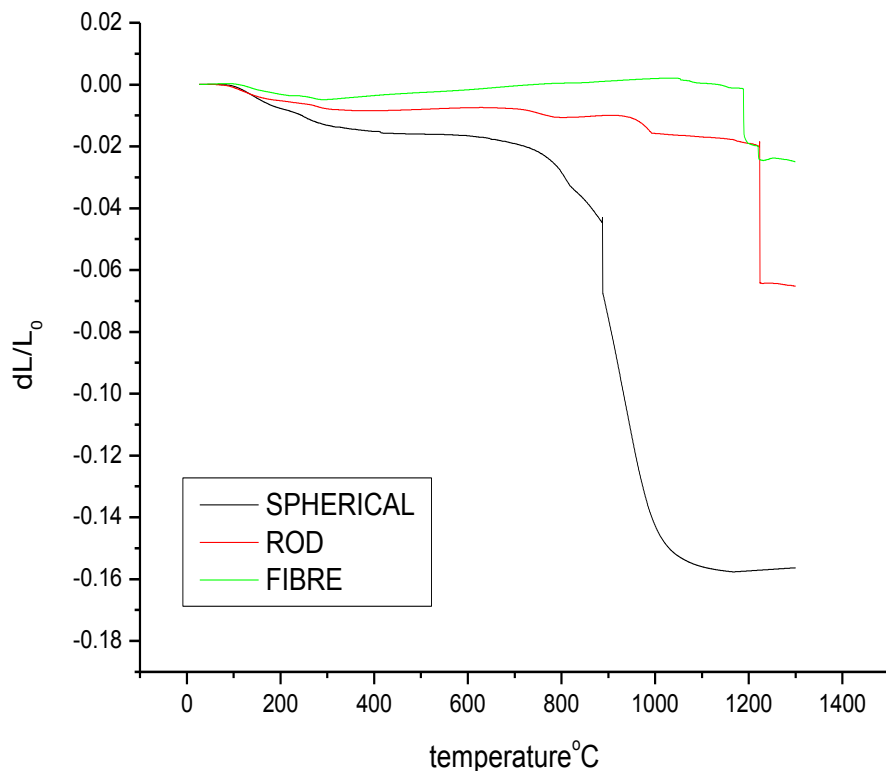


Figure 10 Dilatometric study of Nano HA

4.5 SEM ANALYSIS

4.5.1 NANO –SPHERICAL HYDROXYAPATITE

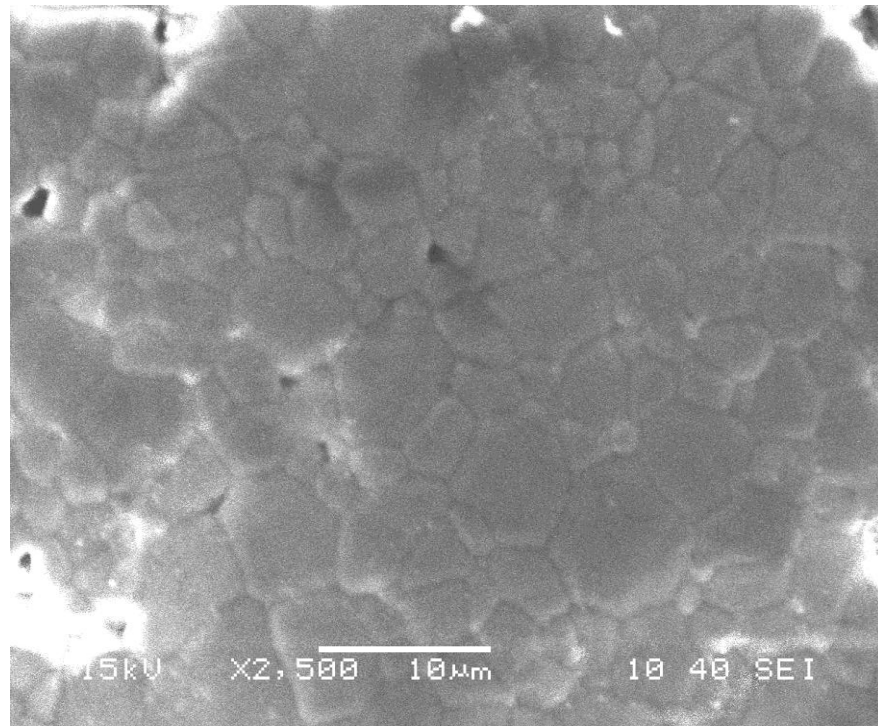


Figure 11 SEM of Sintered Nano-spherical HA at 1250°C

Figure 11 shows the SEM picture of sintered Nano-spherical HA at 1250°C. The microstructure is studied and grain size of the sintered pellet could be estimated to be around 2-3 μm. Grains developed after sintering are found to be with very less pores because of thermal curing. Finally grains can be categorised as dense and with less pores. However pores are arranged and well developed at an average diameter of 2μm.

4.5.2 NANO ROD HYDROXYAPATITE

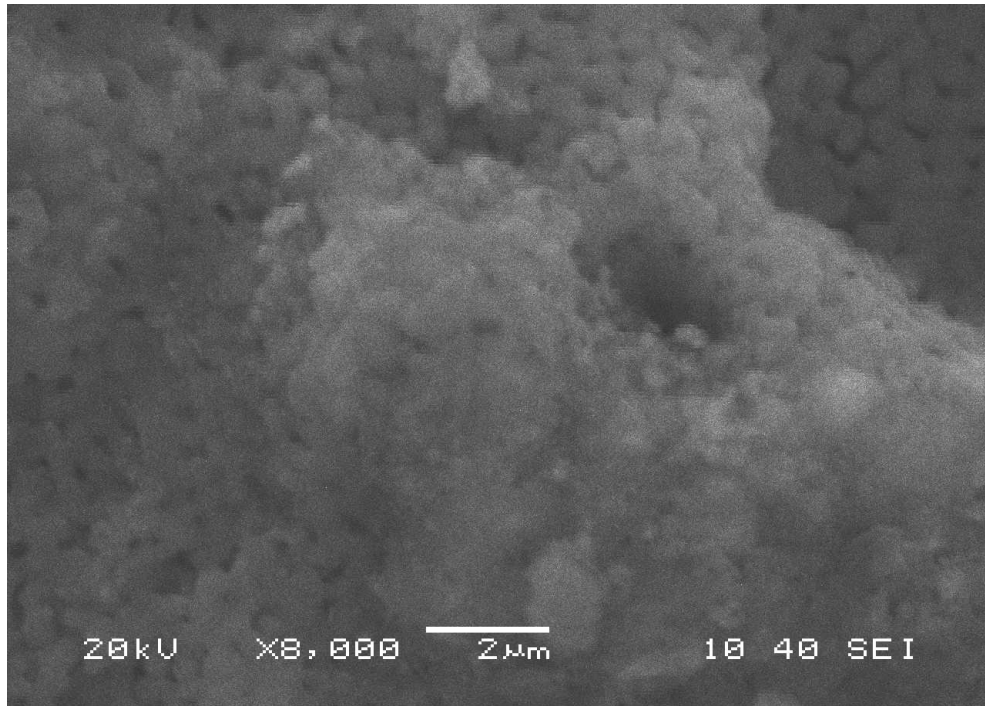


Figure 12 SEM of sintered Nano-spherical HA

Figure 12 shows the SEM picture of sintered Nano-Rod HA at 1000°C. The microstructure is studied and grain size of the sintered pellet could be estimated to be around 1-2 μm . Grains developed after sintering are found to be with very less pores because of thermal curing. Finally grains can be categorised as dense and with less pores. However pores are arranged and well developed at an average diameter of 1 μm .

4.5.3 NANO FIBRE HYDROXYAPATITE

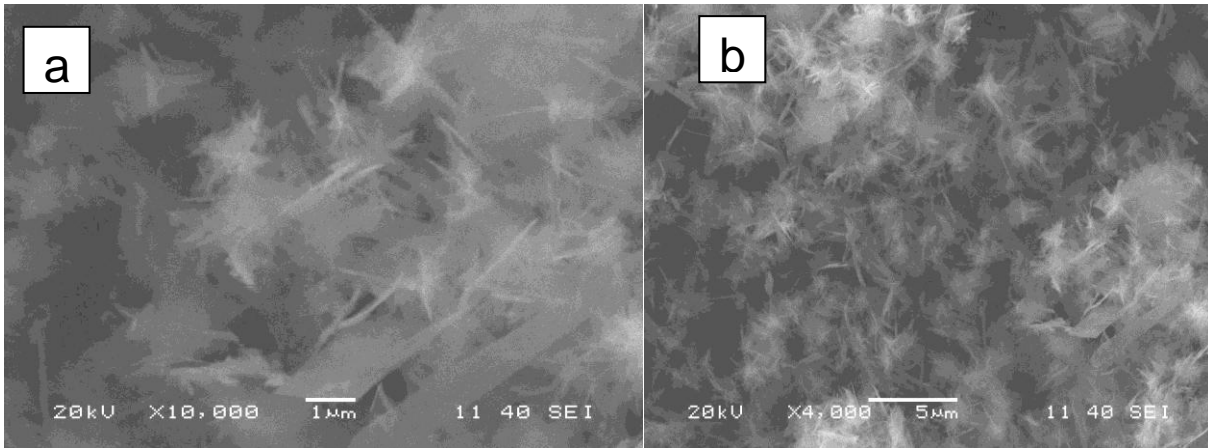


Figure 13 (a) SEM of calcined Nano-fibre HA (b) SEM of raw Nano-fibre HA

Figure 13(a) shows the SEM picture of calcined Nano-fibre HA at 700°C. The microstructure is studied and grain size of the sintered pellet could be estimated to be around 0.5-1 μm. Grains developed after sintering are found to be with very less pores because of thermal curing. Finally grains can be categorised as dense and with less pores when compared to the figure 13(b) of raw nano-fibre HA which is found to be less dense and more porous. However pores are arranged and well developed at an average diameter of 0.5 μm after calcination.

4.6 BULK DENSITY OF DIFFERENT MORPHOLOGIES

Figure 14 shows the relative densification behaviour of the three concerned morphologies

(a) Nano-spherical HA: -At 700°C the density is 1.37gm/cc densification is fast at initial stages upto a temperature of 1000°C. then the rate of densification slows down and final density of 2.88gm/cc is achieved that is 92.02% of the theoretical density.

(b) Nano-rod HA: -At 700°C the density is 1.484 gm/cc densification is slow at initial stages and the rate of densification remains almost constant achieving a density of 2.76gm/cc that is 88.17 % of theoretical density.

(c) Nano-fibre HA :-At 700°C the density is 1.25 gm/cc densification is at a relatively constant rate and finally a density of 2.07gm/cc is achieved that is 66.13 % of theoretical density.

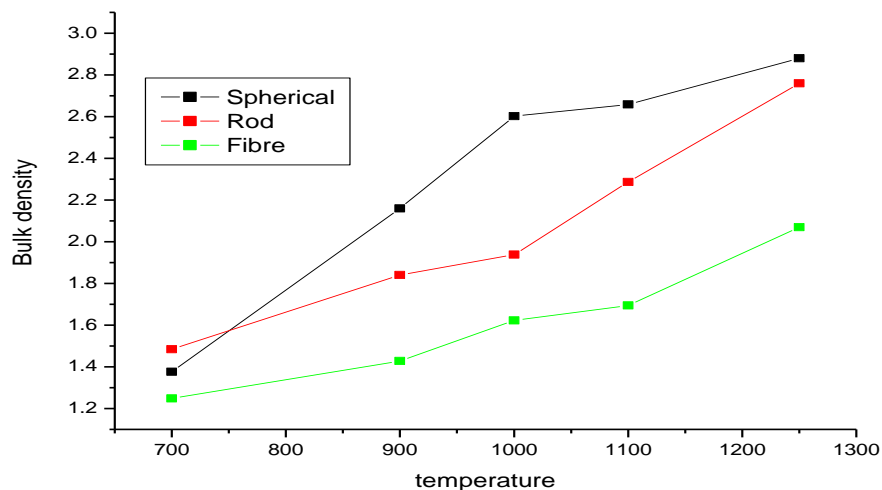


Figure 14 BD composite of HA

4.7 APPARENT POROSITY OF DIFFERENT MORPHOLOGIES

Figure 15 shows the pore formation behaviour of the three concerned morphologies

(a) Nano-spherical HA :- densification is fast at all stages upto a temperature of 1250°C reducing the porosity, and final porosity of 5 % is achieved.

(b) Nano-rod HA :- densification is slow at initial stages and the rate of densification remains almost constant which hardly affects the rate of % porosity achieving a porosity of 5%.

(c) Nano-fibre HA :- Initial porosity being 58% densification goes at a relatively constant rate and finally a porosity of 30% is achieved.

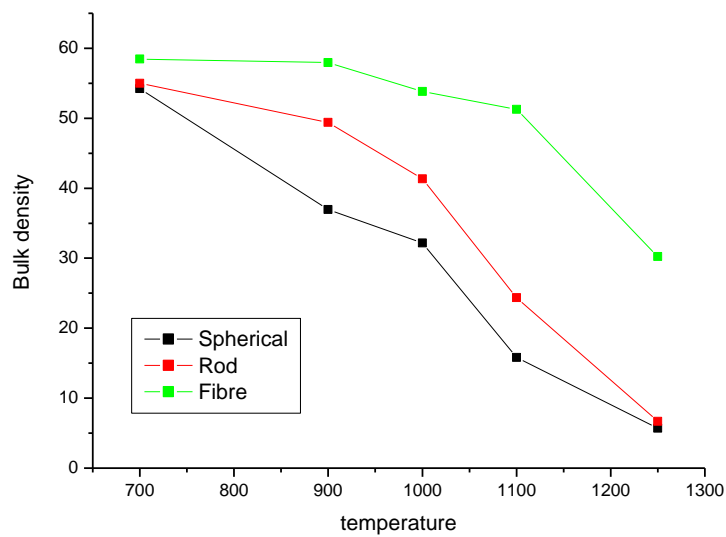


Figure 15 AP composite of HA

4.8 BULK DENSITY AND APPARENT POROSITY AS A FUNCTION OF TEMPERATURE

4.8.1 NANO SPHERICAL HYDROXYAPATITE

Figure 16 shows that the bulk density is found to increase with increasing sintering temperature. This is due to the increase in densification of samples with increase in temperature. Simultaneously the apparent porosity is found to show reverse properties against bulk density and decreases with increase in sintering temperature.

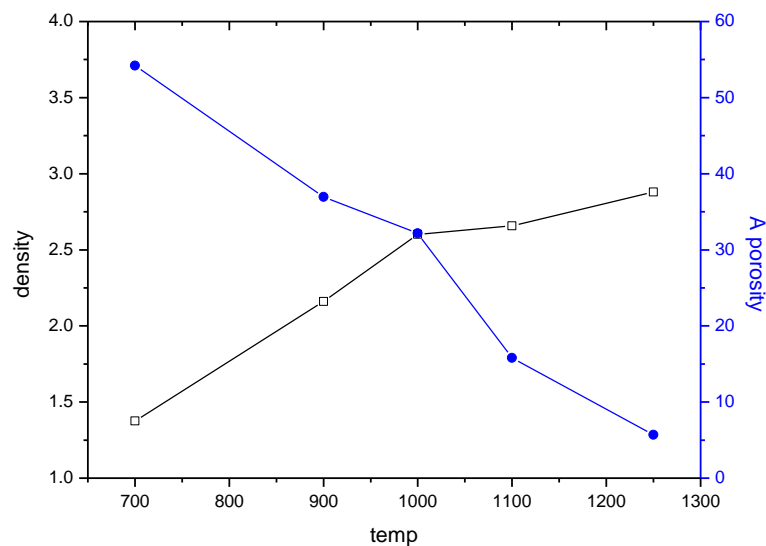


Figure 16 BD vs AP of Nano-spherical HA

4.8.2 NANO ROD HYDROXYAPATITE

Figure 17 shows that the bulk density is found to increase with increasing sintering temperature. This is due to the increase in densification of samples with increase in temperature. Simultaneously the apparent porosity is found to show reverse properties against bulk density and decreases with increase in sintering temperature.

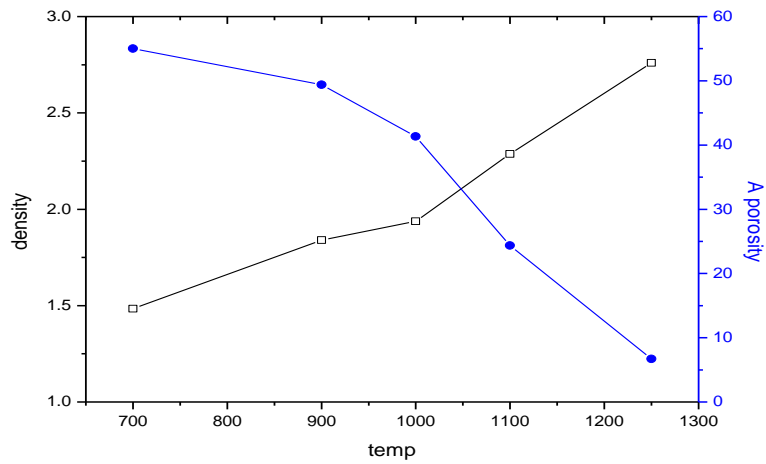


Figure 17 BD vs AP of Nano-rod HA

4.8.3 NANO FIBRE HA

Figure 18 shows that the bulk density is found to increase with increasing sintering temperature. This is due to the increase in densification of samples with increase in temperature. Simultaneously the apparent porosity is found to show reverse properties against bulk density and decreases with increase in sintering temperature.

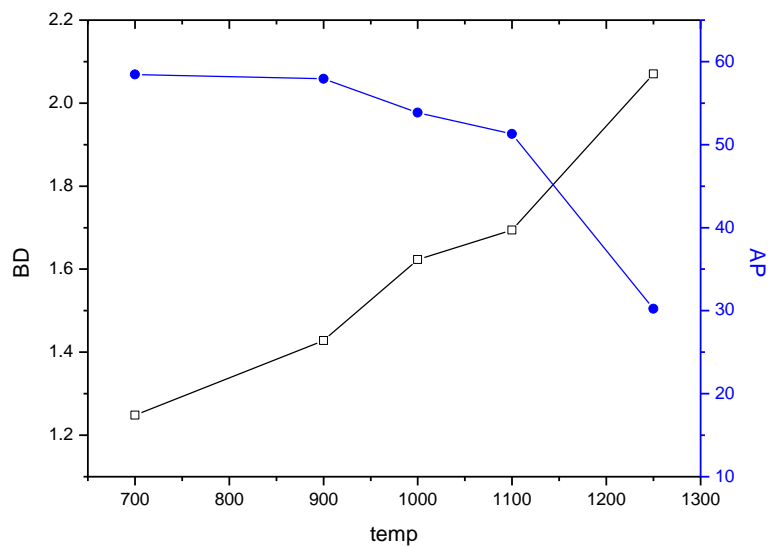


Figure 18 BD vs AP of Nano-fibre HA

Chapter 5

CONCLUSION

A brief conclusion could be summarized as follows:

- [1] Presence of exothermic and endothermic peaks during thermal analysis shows the weight loss of 12 % for nano-spherical and 18% for nano-fibre.
- [2] Hydroxyapatite phase stability was strictly depended on morphology.
- [3] FTIR data reveals the presence of carbonate incorporated which tends to form broad exothermic peaks on thermal analysis. Presence of PO_4^{2-} are also present with OH^- .
- [4] Shrinkage study by dilatometric test up to 1250°C showed 16%, 3% and 2% shrinkage for nano-spherical, nano-rod and nano-fibre, respectively.
- [5] SEM analysis showed the microstructural changes occurring after sintering on all the three morphologies
- [6] Nano-spherical HA is being the most stable towards decomposition and 92.01 % relative density achieved at temperature of 900°C and porosity of 5%.
- [7] Nano-rod HA was moderate stable, which was decomposed and densified to 88.1 % of theoretical density at temperature of 1000°C and porosity of 5%.
- [8] Nano-fibre HA was relatively unstable and decomposed to TCP at early stage and densified to 66.13% of theoretical density at 700°C and porosity of 30 %.
- [9] As the sintering temperature increases nano-spherical HA shows the maximum densification followed by nano-rod and nano-fibre.

REFERENCES

- [1] en.wikipedia.org/wiki/File:Mineraly.sk_-_hydroxylapatit.jpg
- [2] Elliot, J. C. Structure and Chemistry of the Apatites and Other Calcium Orthophosphates, Elsevier, 1994.
- [3] V.S. Komlev, S.M. Barinov, E. Girardin, S. Oscarsson, F. Rustichelli, V.P. Orlovskii, Porous Spherical HA granules, processing and characterization. *Volume 4, Issue 6*, November 2003, Pages 503–508
- [4] P. Ramnarayanan, University of Rochester, Dept of Chemical Engineering, OPT 407 Practical Electron Microscopy Spring 2010.
- [5] Dr. Jon Binner and Mr. Rod Sambrook, Ceramic foams Processing and applications as filter, inter penetrating composites and biomedical M
- [6] S. Laasri, M. Taha, A. Laghzizil, E.K. Hlil, J. Chevalier d, The affect of densification and dehydroxylation on the mechanical properties of stoichiometric HA bioceramics, *Materials Research Bulletin* 45 (2010) 1433–1437.
- [7] S. Ramesh, C.Y. Tan, S.B. Bhaduri, W.D. Teng, Rapid densification of nanocrystalline HA for biomedical applications, *Ceramics International* 33 (2007) 1363–1367
- [8] A. Banerjee, A. Bandyopadhyay, Susmita Bose, HAnanopowders: Synthesis, densification and cell–materials interaction, *Mater. Sci. Engg. C* 27 (2007) 729–735
- [9] P. Cheang, K.A. Khor, Effect of particulate morphology on the tensile behaviour of polymer/HA composites, *Materials Science and Engineering A* 345 (2003) 47–54.

- [10] S.ImanRoohani-Esfahani, Saied Nouri-Khorasani ,Zufu Lu, Richard Appleyard,HalaZreiqat, The influence HA nanoparticle shape and size on the properties of biphasic calcium phosphate scaffolds coated with HA PCL Composites, *Biomaterials* 31 (2010) 5498-5509.
- [11] E. Landi, A. Tampieri , G. Celotti, S. Sprio, Densification behaviour and mechanisms of synthetic HAs, *Journal of the European Ceramic Society* 20 (2000) 2377-2387
- [12] I H. Arita, David S. Wilkinson, Maria Antonieta Mondragnt and Victor M. Castafio, Chemistry and sintering behaviour of thin HA ceramics with controlled porosity,*Biomoteriols*16(1995) 403-408.
- [13]. G. Muralithran, S. Ramesh. The effects of sintering temperature on the properties of HA. *Ceramics International* 26 (2000) 221-230
- [14]. S.K.Swain.S.V.Dorozkin,D. Sarkar,Synthesis and dispersion of HAnanopowders, *Materials Science and Engineering*: Available online 30 March 2012
- [15]. V. Jokanovi, B. Jokanovi , D. Markovi , V. Zivojinovi, S. Pasali , D. Izvonar, M. Plavsi, Kinetics and sintering mechanisms of hydro-thermally obtained HA, *Mater. Chem. Phy.* 111 (2008) 180–185.
- [16]. Gultekin Go ller ,FaikNuzhetOktar , Sintering effects on mechanical properties of biologically derived dentine HA, *Mater. Lett.* 56 (2002) 142–147
- [17] Kaneda, K. et al. *J. Am. Chem. Soc.* **2002**, *124*, 11572.